Zinc sulfide nanoparticles by the pulsed plasma in liquid

E. Omurzak[A*], T. Mashimo[B], S. Sulaimankulova[C]

Priority Organization for Innovation and Excellence, Kumamoto University[A]

Shock Wave and Condensed Matter Research Centre, Kumamoto University[B]

Institute of Chemistry and Chemical Technology, Kyrgyzstan[C]

**Corresponding author's e-mail address: emil@kumamoto-u.ac.jp*

Synthesis of wurtzite-type ZnS nanoparticles by an electric discharge submerged in molten sulfur is reported. By the pulsed plasma between two zinc electrodes of 5 mm diameter in molten sulfur, we have synthesized high-temperature phase (wurtzite-type) ZnS nanocrystals with an average size of about 20 nm. Refined lattice parameters of the synthesized wurtzite-type ZnS nanoparticles were found to be larger than those of the reported ZnS (JCPDS 36-1450). UV-Visible absorption spectroscopy analysis showed that the absorption peak of the as-prepared ZnS sample (319 nm) displays a blue-shift comparing to the bulk ZnS (335 nm). Photoluminescence spectra of the samples revealed peaks at 340, 397, 423, 455 and 471 nm, which were related to excitonic emission and stoichiometric defects.

1. Introduction

Electric discharge based synthesis methods have proven to be non-toxic, low temperature, simple and promising process for various nanomaterials production. So far, the application of electric discharge for the sulfides was only in the form of assisting process or for purposes other than synthesis (such as coating or sintering). FeS coating was deposited on steel substrate using nano-sized FeS powder as starting material and argon as atmosphere by plasma spraying equipment, where plasma was utilized for coating purpose only [1]. Lithium sulfide – carbon (Li_2S-C, Li_4SiS_4-La_2S_3) composite material was prepared using mechanical ball-milling and then were sintered by spark-plasma-sintering (SPS) process, where plasma was used for making better bonding between lithium sulfide and carbon [2, 3]. Recently, synthesis of Bi and Sb sulfides using electric discharge assisted mechanical milling was reported [4]. Also, indium sulfide (In_2S_3) thin film was prepared by plasma-assisted co-evaporation technique, where the indium was supplied by thermal evaporation of indium, while the sulfur was activated using inductively coupled plasma treatment of H_2S gas [5]. Synthesis of metal sulfides by anode discharge electrolysis under argon atmosphere at 723 K was reported [6], which is quite different than the electric discharge (spark, arc, glow, etc) methods, on top of that it requires high-temperature and is a slow process to produce sulfides.

Here we report an electric discharge synthesis method for zinc sulfide nanostructures by using the pulsed plasma in liquid [7]. The method combines physical (spark discharge) and chemical (surrounding liquid) processes that provide us a number of advantages (simple, one-step, low-energy, versatile) for the synthesis of various kinds of

metastable nanomaterials. Possibility of achieving a high-temperature stable phase at very low temperature not only provides economically viable route for applications but also opens a new route to study structural kinetics and chemistry of various nanomaterials.

2. Experimental Details

Experimental apparatus was described in ref [7]. The experimental setup was slightly modified for work with sulfur, which needs to be heated (130 °C) in order to be in liquid state. Duration of a single discharge was measured to be about 10 μs and peak current about 100 A, whereas the input voltage and current were 200 V and 3 A, respectively. The frequency was 60 Hz. Increase of the liquid temperature during the experiment was insignificant due to the short duration of the pulsed discharge and thus no need for cooling of electrodes and/or liquid. For synthesis of ZnS, rod shaped electrodes made from 99.9 % purity zinc rods (Ø5 X 100 mm) were used. Molten sulfur at 140 °C was used as liquid. After applying the pulsed plasma for about 1 hour, the sample was washed out from the sulfur by heated xylene. About 5 grams of powder sample was collected.

3. Results and Discussion

Figure 1 represents the structure refinement result of the XRD profile of the sample produced by the pulsed plasma between two zinc electrodes in molten sulfur: comparison of experimental (solid line) and calculated (dotted line) x-ray powder diffraction patterns for wurtzite ZnS, together with difference plot (below) and expected peak positions (tick marks). The analysis of the profile showed that the produced sample was wurtzite-type ZnS (P63mc, Z=2), matching closely with the JCPDS card No. 36-1450. In addition to wurtzite ZnS, the reflections belonging to metallic Zn were also identified. The diffraction peaks are significantly broadened because of the very small particle size. Profile fitting was done by using 2 phases: wurtzite ZnS and metallic Zn (cubic). Observed reflections were consistent with those of calculated ones and no unindexed reflections could be observed. The constituent phases in the sample was found to be wurtzite ZnS (93.4 vol%) and Zn (metal) (6.6 vol%). Refined unit cell parameters for w-ZnS were a=3.823 Å and c=6.262 Å, which are slightly larger than those of the reported data for w-ZnS (JCPDS Card No. 36-1450). The cell volume of w-ZnS synthesized by this method (79.25 $Å^3$) is larger than the JCPDS standard sample (V=79.11 $Å^3$) for 0.17 %. Slight increase in the lattice parameters might be due to the defects formed during the fast quenching of the plasma state.

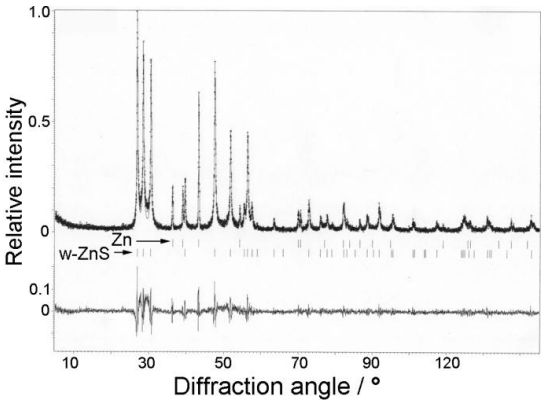

Figure 1. Structure refinement result: comparison of experimental (solid line) and calculated (dotted line) x-ray powder

diffraction patterns for wurtzite ZnS, together with difference plot (below) and expected peak positions (tick marks).

Figure 2 (a) shows the TEM image of the as-prepared sample and (b) the Energy Dispersive X-ray (EDX) spectrum of the particles, c-d) HRTEM images of the nanoparticles with stacking faults denoted with an arrow, e) schematic illustration of the stacking sequence fault in the particle shown in (c). The particles are in the spherical shape but the sizes are not uniform due to the non-equilibrium state of the plasma zone, where the nanoparticles are formed. Some particles were observed in the form of aggregation of small particles that formed bigger size. The particles with less than 20 nm in size dominated. EDX spectrum of the particles revealed that the chemical composition of the produced sample consists of zinc and sulfur elements, which made up ZnS with a stoichiometry of about 1:1. Lattice image of the nanoparticle of about 5 nm in size (Fig. 2c) displayed stacking fault. We can see that the hcp stacking ...ABCABCABC... is disturbed by the removal of a lattice plane C. An intrinsic stacking-fault is created with the new stacking ...ABCAB|ABCA... Stacking faults, denoted by arrows in the HRTEM images, were found in a significant number of particles. In fact, the presence of the defects in the crystals make easier to dope the sample with transition metals in low temperatures in order to achieve desired luminescence. The pulsed plasma in liquid is a non-equilibrium system, where the formation of the nanocrystals accompanied by formation of defected sites, stacking faults.

UV-Visible absorption spectra, represented in Figure 3, show that the absorption peak of the as-prepared w-ZnS sample (319 nm) display a blue-shift compared to the bulk ZnS (335 nm). ZnS nanowires with diameters of 10−25 nm and lengths about 5−8 μm also showed an absorption peak centered at 312 nm [8] and was ascribed to the quantum confinement.

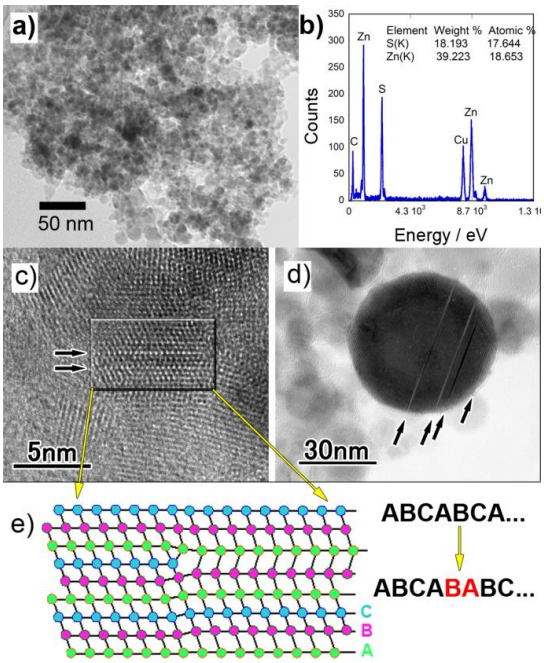

Figure 2. shows: a)TEM image of the as-prepared sample, b) EDX spectrum of the particles, (c,d) HRTEM images of the nanoparticles with stacking faults denoted with an arrow, and e) schematic illustration of the stacking sequence fault in the particle shown in (c).

Room temperature photoluminescence (PL) spectra of the samples using excitation wavelength of 290 nm is given in Figure 3. As we can see that PL spectra of the sample produced by this method showed emissions in the UV (about 340 nm) and visible (400, 425, 450, 470 nm) wavelengths. In the literature, the peak values for the different

kinds of the samples varied depending on the synthesis method.

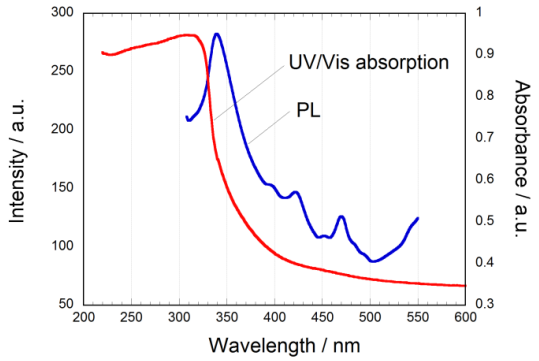

Figure 3. UV/Visible absorption and room temperature photoluminescence spectra of the as-synthesized ZnS nanoparticles.

ZnS nanowires by the pulsed laser vaporization showed emission peak at 3.75, 3.68, 3.06, 2.86, 2.66 eV (330, 337, 405, 433, 466 nm, respectively) and were attributed to the UV excitonic emissions and stoichiometric vacancies and interstitial impurities [9]. Thus, the emission peaks in the visible spectrum of our w-ZnS nanoparticles, centered at 400, 425, 450, and 470 nm, can be related to interstitial sulfur, interstitial zinc, sulfur and zinc vacancies respectively. The emission at 340 nm is related to the UV excitonic emission. The Stokes shift for the ZnS sample is about 20 nm, as it can be seen from Fig. 3.

4. Conclusions

A new simple catalyst-free low-temperature method for the synthesis of the wurtzite structure ZnS nanoparticles of an average size of 20 nm with a spherical shape was presented. By the Rietveld refinement, the structure of the produced ZnS sample was confirmed to match with that of the reported wurtzite-type ZnS (JCDPS 36-1450). Refined lattice volume of the synthesized wurtzite-type ZnS nanoparticles were found to be slightly larger (0.17 %) than that of the JCPDS standard sample. UV-Visible absorption spectroscopy analysis showed that the absorption peak of the as-prepared ZnS sample (319 nm) display a blue-shift compared to the bulk ZnS (335 nm). Photoluminescence spectra of the samples revealed peaks at 340, 397, 423, 455 and 471 nm, which were related to excitonic emission and stoichiometric defects.

REFERENCES

[1] Y. Xu *et al.*, *J. Mater. Sci. Technol*. **22**, 589 (2006).

[2] T. Takeuchi *et al.*, *J. Power Sources*, **195**, 2928 (2010).

[3] Z. Liu *et al.*, *Mater. Lett*., **62**, 1366 (2008).

[4] A. Calca *et al.*, *J. Alloy. Compd*., **455**, 285 (2008).

[5] S. Kosaraju *et al.*, *Sol. Energ. Mat. Sol. Cells*, **90**, 1121 (2006).

[6] T. Oishi *et al.*, *Electrochemistry*, **70**, 697 (2002).

[7] E. Omurzak *et al.*, *J. Nanosci. Nanotechnol*., ***7***, 3157 (2007).

[8] Y. Ding *et al.*, *Chem. Phys. Lett*., **398**, 32 (2004).

[9] Q. Xiong *et al.*, *Nano Lett*., **4**, 1663 (2004).